Quantifying Seismically-Induced Landslide Susceptibility in Puerto Rico for Disaster Preparedness

Elvin Cordero

Affiliation:

- Department of Marine Sciences, University of Puerto Rico-Mayagüez, Marine Geology Lab, Isla Magueyes, Lajas, Puerto Rico 00667

- Puerto Rico Seismic Network, University of Puerto Rico-Mayagüez, Universidad de Puerto Rico Edificio D Mayagüez, Puerto Rico 00680

Email: elvin.cordero@upr.edu

Research Domain: Natural Hazards, GIS, Remote Sensing

Funding Information:

Date: February 17, 2024

Keywords: Hazus, Landslide Susceptibility, Earthquake, Risk Analysis

DRAFT

1 Introduction

Puerto Rico, a region profoundly influenced by its intricate geological and seismic profile, serves as a critical case study for analyzing natural hazards within the Caribbean. This territory, situated at the juncture of the North American and Caribbean tectonic plates, is inherently prone to a spectrum of seismic activities, from subtle tremors to profound earthquakes. Such seismic dynamics significantly heighten the propensity for slope instabilities, leading to landslides that threaten both human settlements and infrastructural integrity. The cataclysmic events of the 2020 southwestern Puerto Rico earthquakes have starkly highlighted the exigency of evaluating landslide susceptibility under seismic influences.

This research delves into the seismic genesis of landslides in Puerto Rico, combining a multidisciplinary synthesis of geotechnical, spatial, and historical analyses to dissect the underlying mechanisms of slope failures triggered by earthquakes.

Central to this study is the integration of key determinants of landslide susceptibility—seismic intensity, peak ground velocity, slope gradient, lithological characteristics, and hydrological dynamics—leveraging the predictive framework posited by Nowicki Jessee et al. (2018) (2). Through the application of this model, we aim to quantitatively assess and model the susceptibility landscape of Puerto Rico to seismically induced landslides, employing the model at a higher resolution.

Using the Nowicki Jessee et al. (2018) model, probability of landsliding can be predicted using a linear combination of individual predictor variables including peak ground velocity (PGV), slope, lithology, land cover, and a compound topographic index (CTI) to express a logistic function:

$$Logit(P) = \ln\left(\frac{P}{1-P}\right) = t, \tag{1}$$

$$t = a + b * \ln(pgv) + c * slope + d * lithology + e * landcover + f * cti + g * \ln(pgv) * slope, \tag{2}$$

$$P(t) = \frac{1}{1+e^{-t}}, \tag{3}$$

Where a,b,c,d,e,f and g are coefficients solved for within the Nowicki Jessee et al. (2018) model, and pgv represents peak ground velocity and cti is the compound topographic index.

The overarching goal is to develop a predictive model for landslide susceptibility in Puerto Rico using the Nowicki Jessee et al. (2018) model. By advancing the granularity of our understanding of landslide dynamics in response to seismic stimuli, this study aspires to fortify Puerto Rico's resilience against such inevitable natural adversities, ensuring a proactive posture in landslide risk anticipation and management. Such a model not only advances our scientific understanding of landslide dynamics but also serves as a crucial tool for disaster risk management, land-use planning, and the development of mitigation strategies to protect vulnerable communities. Through this research, we contribute to a safer and more resilient Puerto Rico, where the risks of seismically induced landslides are understood, anticipated, and managed.

2 Methodology

2.1 Study Region

Puerto Rico, along with the Virgin Islands and eastern Hispaniola, exist on a microplate in an active plate boundary zone that lies between the westward-moving North America Plate and the eastward-moving Caribbean Plate, marked by the Anegada Trough and Muertos Trough to the south and the Puerto Rico Trench to the north (O'Loughlin and Lander 2003). There are complex motions occurring between Puerto Rico and the Dominican Republic, where to the south, in Mona Passage and Mona Canyon, there is extension and oblique thrusting, while possible strike-slip motion is happening in the Puerto Rico Trench (Mercado and McCann (1998); Fig. 3). The interpolate motion, running parallel of the Puerto Rico Trench, averages two meters per century and slow subduction zones can generate interpolate-thrust earthquakes and associated tsunamis (Atwater et al. 2014). Mona Canyon is the location of the most important tsunamigenic sources near northwestern Puerto Rico, where the sea floor lies more than 2 km lower than its surrounding due extensional tectonics which has caused the down dropping of large blocks of the inner wall of the trench, resulting in the development of normal faults (Mercado and McCann 1998).

2.2 Software

The geospatial processing procedures were completed with the R statistical language (R Core Team 2023) using spatial toolsets such as the *terra* and *tidyterra* packages (Hijmans 2023; Hernangómez 2023). Polygon drafting and editing was done in the QGIS geographic information system software (QGIS Development Team 2024).

2.3 Model Inputs

2.3.1 Peak Ground Velocity (PGV)

Peak Ground Velocity (PGV) measures the maximum speed at which the ground moves at a location during an earthquake, typically expressed in terms of distance per unit time. It is a critical parameter in seismology and earthquake engineering, indicating the intensity of ground motion and its potential to cause structural damage and induce landslides. PGV is used alongside peak ground acceleration (PGA) and spectral acceleration (SA) in seismic hazard analysis to characterize expected ground shaking, informing the design of earthquake-resistant structures and mitigation strategies. High PGV values are associated with increased risk of severe structural damage and slope failures, making accurate PGV estimation vital for

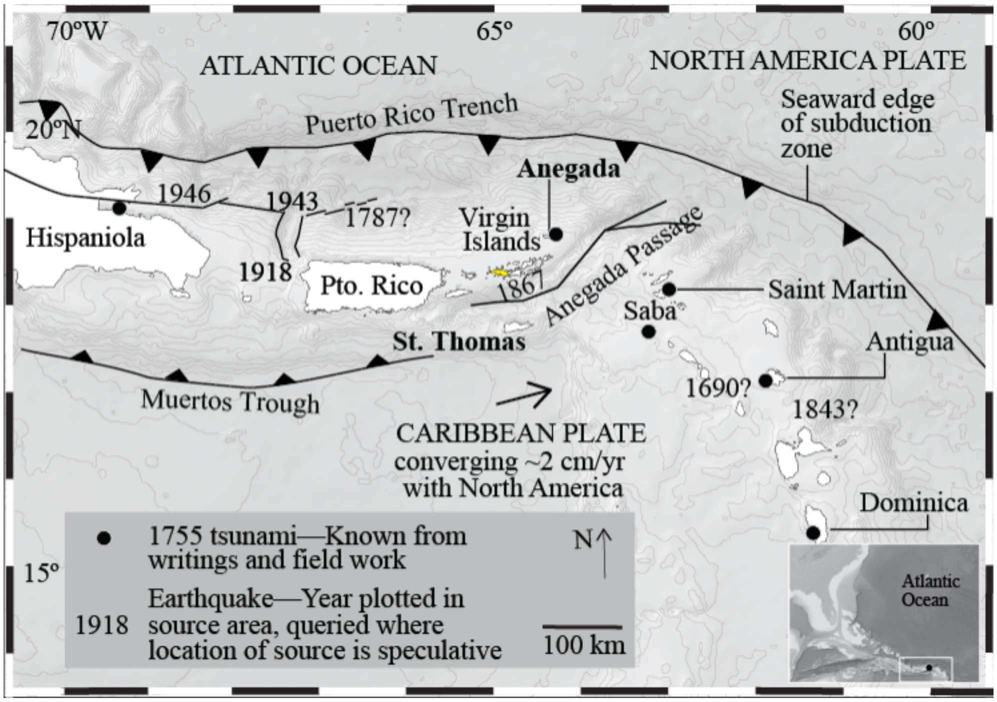

Figure 1: The Puerto Rico-Virgin Islands microplate. Stars represent the four scenarios analyzed by Ramirez-Rivera (2016): 1787 Puerto Rico Trench (1787PRT), 1867 Virgin Islands Basin (1867 VIB), 1918 Mona Canyon (1918 MC), and the hypothetical event 13PR. Source: Ramirez-Rivera (2016), Figure 1.2, pg 6.

risk assessments, building codes, and the development of earthquake preparedness measures. The PGV modeled for three historical earthquake scenarios were used by Ramírez-Rivera (2016) to estimate earthquake loss; these included the M7.5 Mona Canyon earthquake of 1918, the M7.5 Virgin Island Basin (VIB) earthquake of 1867, and the M~8.0 event that occurred offshore the northern coast of Puerto Rico on May 2, 1787 (Doser et al. 2005). Specified fault geometry and magnitude of the earthquake scenarios from estimates of i) fault dimensions, ii) intensity map, and iii) ground motion were obtained by Ramírez-Rivera (2016) from the literature (Mercado and McCann 1998; Huérfano 2003; Zahibo et al. 2003). The maximum PGV possible at a given location was used for the analysis. This was grouped into equal intervals ranging from 0-5 and >50 cm/s, each assigned a landslide susceptibility score between zero and 10, from none to very high.

2.3.2 Terrain Analysis

Digital Elevation Models (DEMs) are pivotal in landslide susceptibility analysis, through precise slope gradient calculations and hydrological modeling. DEMs delineate steep terrains at heightened landslide risk and areas susceptible to water-induced soil destabilization. By integrating DEMs with geotechnical data, researchers can quantitatively assess erosion dynamics and structural stability of landforms. The SRTM15+ global bathymetry and topography (15-arc sec resolution) for Puerto Rico was downloaded using the *elevatr* package (Tozer et al. 2019; Hollister et al. 2023). Slope, α, was calculated using the Fleming and Hoffer (1979) method and eight neighboring cell. Flow direction of water, Q_d for each cell was estimated from the direction of the greatest drop in elevation (Hijmans 2023) and flow accumulation, A_s, was defined as the sum of flow directions of the surrounding neighbors (Equation 4).

$$A_s = \sum_{n=1}^{8} Q_d \tag{4}$$

With DEM-derived flow accumulation as a proxy for specific basin area and the slope in radians, the compound topography index (CTI) (Moore et al. 1991), also known as the topographical wetness index (TWI), was computed using Equation 5.

$$CTI = \ln\left(\frac{A_s}{tan(\alpha)}\right) \tag{5}$$

The slope angle (degrees) were given landslide susceptibility scores according to the Nadim et al. (2006) categorization of slope data. The CTI was grouped into equal intervals ranging from 0-5 and >50, each assigned a landslide susceptibility score between zero and 10, from none to very high.

2.3.3 Land Cover

Land cover significantly influences landslide susceptibility through its modulation of surface hydrological dynamics and slope stability mechanisms. Vegetation, particularly forest cover, enhances soil cohesion via root systems and mitigates surface runoff by facilitating water infiltration, thereby reducing hydraulic pressures on slope materials. Conversely, impervious surfaces amplify runoff, potentially escalating hydraulic stress at slope bases and along drainage paths, increasing susceptibility to landslides. Anthropogenic land cover alterations, such as deforestation and urban development, disrupt natural drainage systems and compromise slope integrity by reducing vegetative stabilization and altering load distributions. Moreover, land cover changes affecting soil erosion rates can directly impact slope stability by modifying soil support and contributing to the accumulation of destabilizing sediments. Regional land cover dataset for Puerto Rico was downloaded from the National Oceanic and Atmospheric Administration's (NOAA) Coastal Change and Analysis Program (CCAP) at 30-m resolution (NOAA, Office For Coastal Management). The CCAP dataset was reclassified following the definitions in the Global Land Cover Map for 2009 (GlobCover2009) (Arino et al. 2012). The landslide susceptibility score was assigned by rating the land cover type from one to 10, from very low to very high.

2.3.4 Lithology

Lithology is pivotal in assessing an area's susceptibility to seismically induced landslides, influencing both the mechanical strength and the hydrological behavior of geological materials in response to earthquake forces. The inherent properties of different rock types, such as cohesion, permeability, and susceptibility to weathering, determine their stability under seismic shaking. Weak, unconsolidated, or highly fractured lithologies are particularly prone to slope failures during earthquakes, while lithological contrasts can create potential slip planes. Additionally, certain rock types can amplify seismic waves, further exacerbating landslide risk. Understanding the lithological framework is, therefore, essential for accurate landslide susceptibility assessments in seismically active regions, enabling targeted mitigation strategies to minimize earthquake-induced landslide hazards. Using the geologic map of Puerto Rico produced by (1998), the geologic descriptions were grouped by lithology (i.e. endogenous, extrusive, or sedimentary rocks) and stratigraphy (e.g. Cenozoic, Mesozoic, etc.) and assigned a landslide susceptibility score following the Nadim et al. (2006) classification scheme adjusted to fit a scale of one to 10, from very low to very high. The lithology was additionally reclassified into the GLiM (Global Lithological Map) (Hartmann and Moosdorf 2012) lithological categories for use with the Nowicki Jessee et al. (2018) model.

3 Preliminary Results

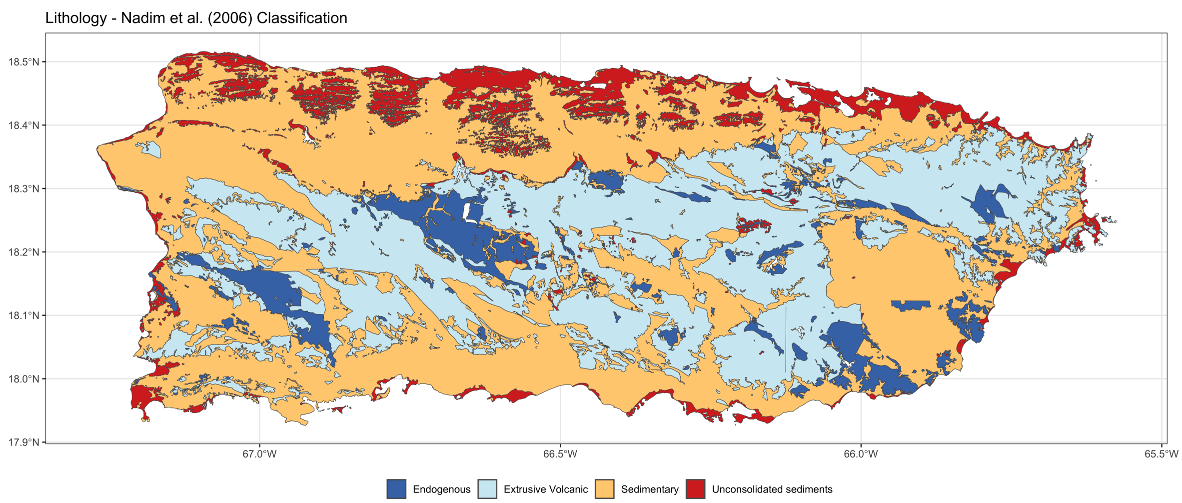

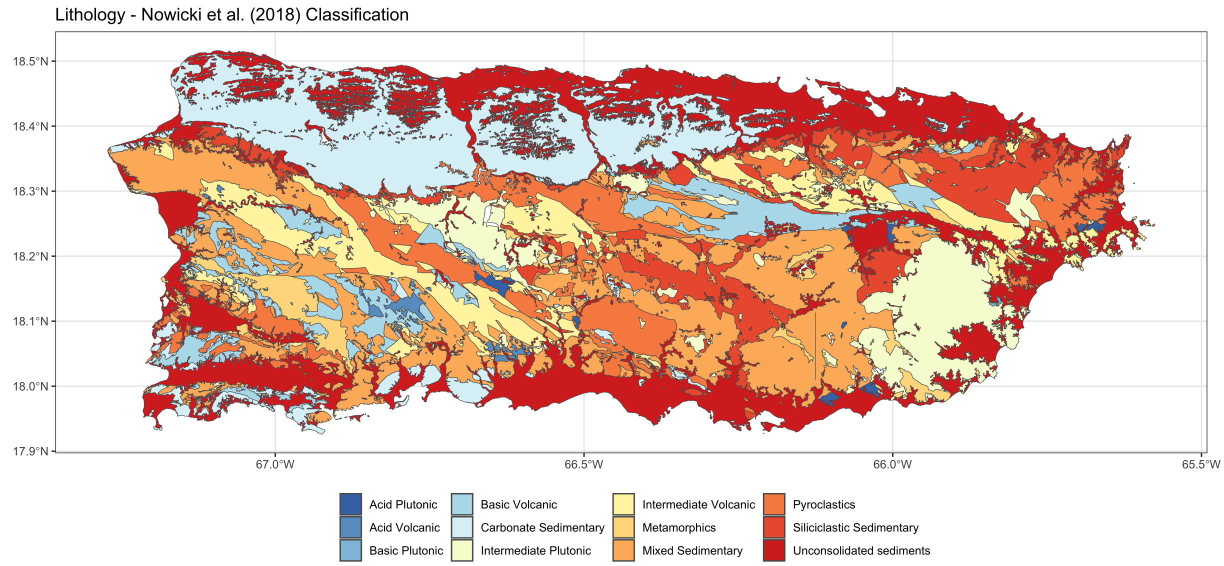
Lithology - Nowicki et al. (2018) Classification
18.5°N
18.4°N
18.3°N
18.2°N
18.1°N
18.0°N
17.9°N
67.0°W
66.5°W
66.0°W
65.5°W
Acid Plutonic
Acid Volcanic
Basic Plutonic
Basic Volcanic
Carbonate Sedimentary
Intermediate Plutonic
Intermediate Volcanic
Metamorphics
Mixed Sedimentary
Pyroclastics
Siliciclastic Sedimentary
Unconsolidated sediments

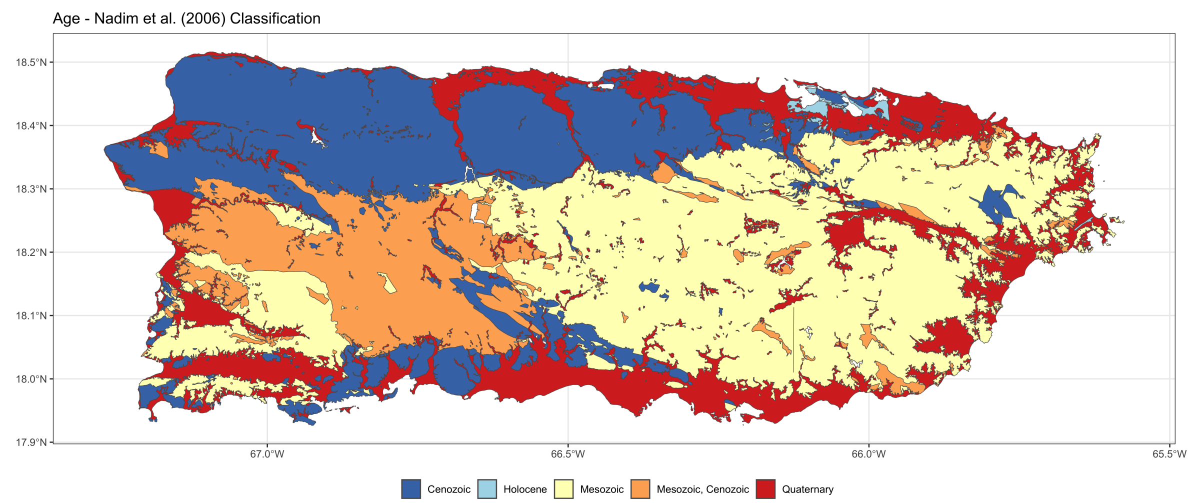
Age - Nadim et al. (2006) Classification
18.5°N
18.4°N
18.3°N
18.2°N
18.1°N
18.0°N
17.9°N
67.0°W
66.5°W
66.0°W
65.5°W
Cenozoic
Holocene
Mesozoic
Mesozoic, Cenozoic
Quaternary

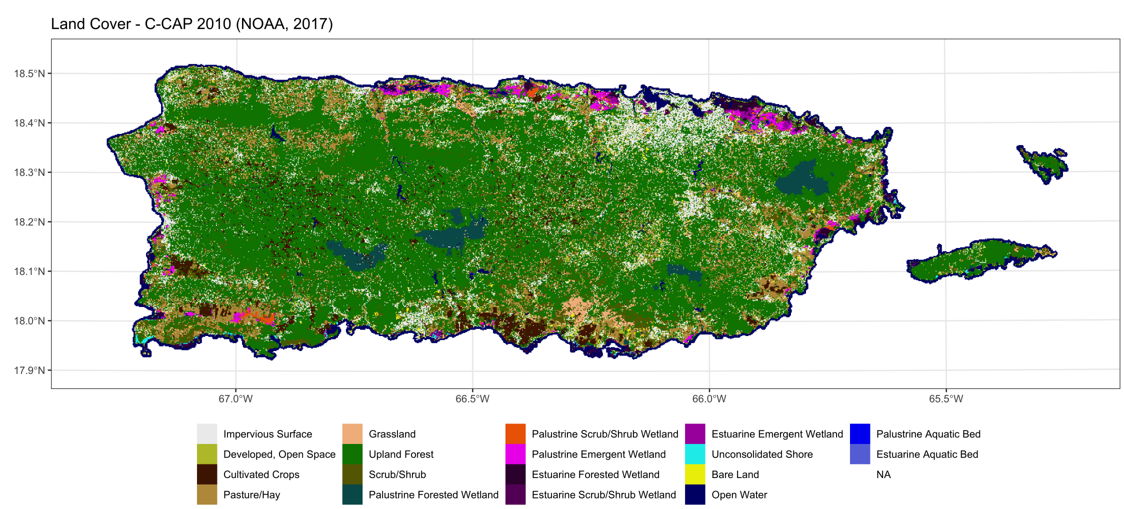
Land Cover - C-CAP 2010 (NOAA, 2017)
18.5°N
18.4°N
18.3°N
18.2°N
18.1°N
18.0°N
17.9°N
67.0°W
66.5°W
66.0°W
65.5°W
Impervious Surface
Developed, Open Space
Cultivated Crops
Pasture/Hay
Grassland
Upland Forest
Scrub/Shrub
Palustrine Forested Wetland
Palustrine Scrub/Shrub Wetland
Palustrine Emergent Wetland
Estuarine Forested Wetland
Estuarine Scrub/Shrub Wetland
Estuarine Emergent Wetland
Unconsolidated Shore
Bare Land
Open Water
Palustrine Aquatic Bed
Estuarine Aquatic Bed
NA

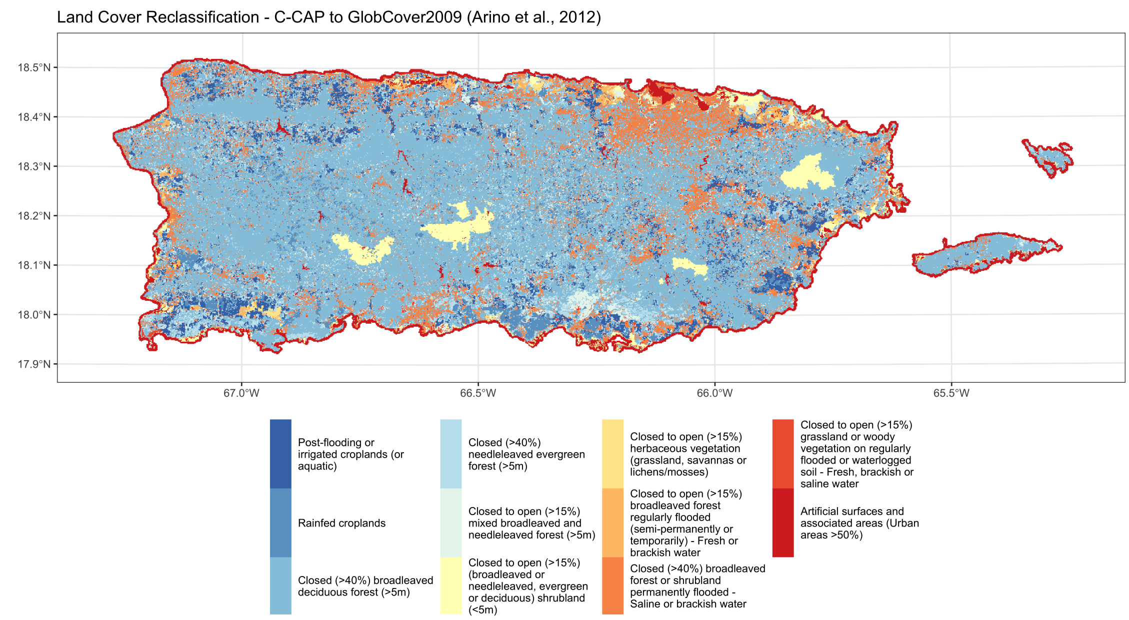
Land Cover Reclassification - C-CAP to GlobCover2009 (Arino et al., 2012)
18.5°N
18.4°N
18.3°N
18.2°N
18.1°N
18.0°N
17.9°N
67.0°W
66.5°W
66.0°W
65.5°W
Post-flooding or irrigated croplands (or aquatic)
Rainfed croplands
Closed (>40%) broadleaved deciduous forest (>5m)
Closed (>40%) needleleaved evergreen forest (>5m)
Closed to open (>15%) mixed broadleaved and needleleaved forest (>5m)
Closed to open (>15%) (broadleaved or needleleaved, evergreen or deciduous) shrubland (<5m)
Closed to open (>15%) herbaceous vegetation (grassland, savannas or lichens/mosses)
Closed to open (>15%) broadleaved forest regularly flooded (semi-permanently or temporarily) - Fresh or brackish water
Closed (>40%) broadleaved forest or shrubland permanently flooded - Saline or brackish water
Closed to open (>15%) grassland or woody vegetation on regularly flooded or waterlogged soil - Fresh, brackish or saline water
Artificial surfaces and associated areas (Urban areas >50%)

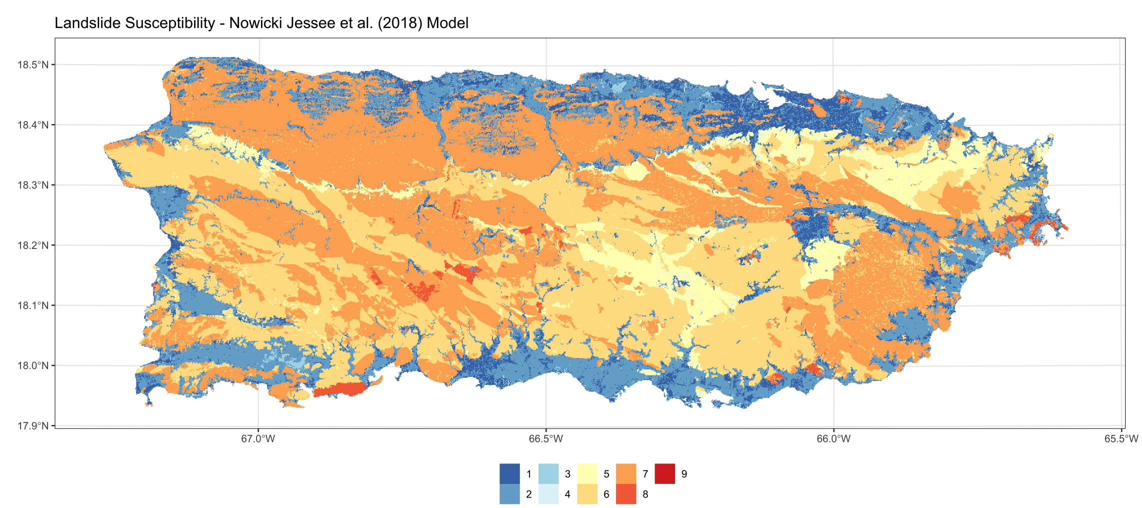
Landslide Susceptibility - Nowicki Jessee et al. (2018) Model
18.5°N
18.4°N
18.3°N
18.2°N
18.1°N
18.0°N
17.9°N
67.0°W
66.5°W
66.0°W
65.5°W
1
2
3
4
5
6
7
8
9

References

(1998) Geology, geochemistry, geophysics, mineral occurrences, and mineral resource assessment for the Commonwealth of Puerto Rico. Prepared in cooperation with the Puerto Rico Department of Natural Resources, University of Puerto Rico at Mayaguez

Arino O, Ramos Perez JJ, Kalogirou V, et al (2012) Global Land Cover Map for 2009 (GlobCover 2009). 40 data points

Atwater BF, Fuentes Z, Halley RB, et al (2014) Effects of 2010 Hurricane Earl amidst geologic evidence for greater overwash at Anegada, British Virgin Islands. Adv Geosci 38:21–30. https://doi.org/10.5194/adgeo-38-21-2014

Doser DI, Rodriguez CM, Flores C (2005) Historical earthquakes of the Puerto Rico–Virgin Islands region (1915–1963). In: Active Tectonics and Seismic Hazards of Puerto Rico, the Virgin Islands, and Offshore Areas. Geological Society of America

Fleming M, Hoffer R (1979) Machine processing of landsat MSS data and DMA topographic data for forest cover type mapping. Laboratory for Applications of Remote Sensing, Purdue University, West Lafayette, Indiana

Hartmann J, Moosdorf N (2012) The new global lithological map database GLiM: A representation of rock properties at the Earth surface. Geochem Geophys Geosyst 13:2012GC004370. https://doi.org/10.1029/2012GC004370

Hernangómez D (2023) Using the tidyverse with terra objects: The tidyterrapackage. JOSS 8:5751. https://doi.org/10.21105/joss.05751

Hijmans RJ (2023) *Terra*: Spatial Data Analysis

Hollister JW, (Ctb) ALR, (Rev) MWB, et al (2023) *Elevatr*: Access Elevation Data from Various APIs

Huérfano V (2003) Susceptibilidad de Puerto Rico ante el efecto de maremotos locales. PhD thesis, University of Puerto Rico-Mayagüez, Department of Marine Sciences

Mercado A, McCann W (1998) Numerical Simulation of the 1918 Puerto Rico Tsunami. Natural Hazards 18:57–76. https://doi.org/10.1023/A:1008091910209

Moore ID, Grayson RB, Ladson AR (1991) Digital terrain modelling: A review of hydrological, geomorphological, and biological applications. Hydrological Processes 5:3–30. https://doi.org/10.1002/hyp.3360050103

Nadim F, Kjekstad O, Peduzzi P, et al (2006) Global landslide and avalanche hotspots.

Landslides 3:159–173. https://doi.org/10.1007/s10346-006-0036-1

NOAA, Office For Coastal Management Coastal Change Analysis Program (C-CAP) Regional Land Cover 30 m Raster Dataset

Nowicki Jessee MA, Hamburger MW, Allstadt K, et al (2018) A Global Empirical Model for Near-Real-Time Assessment of Seismically Induced Landslides. JGR Earth Surface 123:1835–1859. https://doi.org/10.1029/2017JF004494

O'Loughlin KF, Lander JF (2003) Caribbean tsunamis: A 500-year history from 1498-1998. Kluwer Academic Publishers, Dordrecht

QGIS Development Team (2024) QGIS Geographic Information System

R Core Team (2023) *R*: A language and environment for statistical computing

Ramírez-Rivera A (2016) Earthquake loss estimation in puerto rico from historical and potential earthquake scenarios. University of Puerto Rico-Mayagüez, Department of Geology

Tozer B, Sandwell DT, Smith WHF, et al (2019) Global Bathymetry and Topography at 15 Arc Sec: SRTM15+. Earth and Space Science 6:1847–1864. https://doi.org/10.1029/2019EA000658

Zahibo N, Pelinovsky E, Yalciner A, et al (2003) The 1867 Virgin Island tsunami: Observations and modeling. Oceanologica Acta 26:609–621. https://doi.org/10.1016/S0399-1784(03)00059-8